ON THE EFFECT OF THE INTRACELLULAR CALCIUM-SENSITIVE K^+ CHANNEL IN THE BURSTING PANCREATIC β-CELL

TERESA REE CHAY
Department of Biological Sciences, University of Pittsburgh, Pittsburgh, Pennsylvania

ABSTRACT Based on the observation that the calcium-activated K^+ channel in the pancreatic islet cells can also be activated by the membrane potential, we have formulated a mathematical model for the electrical activity in the pancreatic β-cell. Our model contains two types of ionic channels, which are active above the subthreshold glucose concentration in the limit-cycle region: a Ca^{2+}-activated, voltage-gated K^+ channel and voltage-gated Ca^{2+} channel. Numerical simulation of the model generates bursts of electrical activity in response to a variation of k_{Ca}, the rate constant for sequestration of intracellular calcium ions. The period and duration of the bursts in response to k_{Ca} are in good agreement with experiment. The model predicts that (*a*) a combined spike and burst pattern can be created using only single species of inward and outward currents, (*b*) the inactivation kinetics (i.e., h) in the inward current is not a necessary condition for the generation of the pattern, and (*c*) a given pattern or intensity of electrical activity may produce different levels of intracellular Ca^{2+} depending on the set of certain electrical parameters.

INTRODUCTION

The cells in the pancreas that secrete insulin are called β-cells. They are situated in tightly associated cellular aggregates known as the islets of Langerhans. One of the most interesting properties of the β-cell is its ability to exhibit a characteristic electrical activity when glucose is added in the perfusion medium (Dean and Mathews, 1970; Ribalet and Beigleman, 1979; Atwater et al., 1980). In the presence of low glucose concentration (i.e., below 5 mM), the voltage across the plasma membrane of the β-cell remains at the resting level of -68 mV (Ashcroft et al., 1984). When the glucose concentration is raised above ~5.5 mM, however, the membrane potential displays the burst activity. This consists of an active phase during which spikes are generated and a silent phase during which the membrane is hyperpolarized. The burst activity continues until the glucose level reaches ~16.6 mM. Characteristics of the electrical burst, which change appreciably as glucose increases, are the relative duration of the active phase and the burst period; increasing glucose increases the relative duration of the active phase (Beigelman et al., 1977; Meissner and Pressler, 1980; Atwater et al., 1980), while the burst period decreases at first but starts to increase near the glucose saturation level (i.e., 16.5 mM) (Meissner and Schmelz, 1974; Beigelman et al., 1977). In high glucose concentrations (i.e., above 16.6 mM), the burst pattern disappears and spike activity becomes continuous.

Simultaneous measurements of electrical activity in impaled β-cells and insulin release from the corresponding islets (Atwater et al., 1979; Scott et al., 1981) have shown that insulin is released from the β-cell during these bursts. The insulin release rate has a periodicity close to that of the burst of electrical activity. The mechanism involved in the regulation of insulin release has been the subject of extensive investigation.

A large body of evidence suggests that the cytosolic calcium ionic concentration, $[Ca^{2+}]_i$, regulates insulin release. Using the intracellular trapped fluorescent Ca^{2+} indicator quin2, Rorsman et al. (1984) have shown that glucose stimulates an increase of the cytosolic free Ca^{2+} concentration in adult noninbred obese-β-cells. Also, Wollheim and Pozzan (1984) have given direct experimental evidence that in suspension of RINm5F, secretagogue-induced insulin release was accompanied by a rise in $[Ca^{2+}]_i$. Thus, how $[Ca^{2+}]_i$ changes in response to glucose and how the electrical activity controls the level of $[Ca^{2+}]_i$ seem to be a key to understand the insulin release mechanism.

The Ca^{2+}-activated K^+ channel is believed to be an important link between $[Ca^{2+}]_i$ and the bursting electrical activity (Atwater et al., 1979; Petersen and Maruyama, 1984). Based on the existence of this channel and also on evidence that the β-cell possesses both the voltage-gated K^+ channel (Ribalet and Beigelman, 1979) and the voltage-gated Ca^{2+} channel (Matthews and Sakamoto, 1975; Atwater et al., 1980), Chay and Keizer (1983) have proposed a mathematical model for the bursting phenomenon in the electrical activity of the β-cell. This model consists of the following: a potassium channel with a conductance that is activated by the binding of intracellular Ca^{2+}; Hodgkin-Huxley—like conductances for K^+ and

Ca^{2+} (Ca^{2+} replaces Na^+ in the Hodgkin-Huxley model); and a sink for intracellular Ca^{2+} stores, possibly mitochondria, which is activated by glucose (Rorsman et al., 1984). The glucose dependence in the Chay-Keizer model comes in through the rate constant of the efflux of Ca_i.

The advent of the patch-clamp technique for studying the properties of single ionic channels have made possible to characterize a high-conductance K^+ channel, which is activated by intracellular Ca^{2+} ions (Cook et al., 1984; Findlay et al., 1985*b*) and a low-conducatance K^+ channel that is inhibited by a metabolite of glucose (i.e., ATP) and has therefore been called the ATP-inhibited K^+-channel (Cook and Hales, 1984; Ashcroft et al., 1984; Findlay et al., 1985*a*). The low-conductance K^+-channel is insensitive to membrane potential and Ca_i (Findlay et al., 1985*a*), but could be inhibited a glucose concentration $\geq$10 mM (Ashcroft et al., 1984). The experiments of Cook et al. (1984) and Findlay et al. (1985*b*), on the other hand, reveal that the high-conductance K^+ channels in the islet cells can be activated by both membrane potential and cytosolic Ca^{2+} ions. The "open probability" of their K^+ channel suggests further that the voltage-sensitive K^+ channel, which is believed to exist in the β-cell (Atwater et al., 1979), is indeed the high-conductance Ca_i-sensitive K^+ channel, i.e. the V-gated K^+ channel and Ca_i-sensitive K^+ channels are identical.

In this paper, we modify the Chay-Keizer model (which assumes the existence of two separate K^+ channels) and demonstrate that a Ca_i-sensitive K^+ channel that is activated by membrane potential, along with a voltage-gated Ca^{2+} channel, is sufficient to produce the observed steady state bursts of the β-cell electrical activity.

MODEL

In the β-cell, the total ionic current consists of a calcium current, potassium current, and leak current. There are two types of potassium currents: the ATP-inhibited K^+ current $I_{K,ATP}$ and the Ca_i-sensitive K^+ current $I_{K,Ca}$. In the resting state, $I_{K,ATP}$ in the β-cell dominates the resting-cell K^+ permeability (Aschcroft et al., 1984), and this current is primarily responsible for the resting membrane potential of about -70 mV. At this low potential, there is essentially no current flowing through Ca^{2+}-activated K^+ channels and also voltage-gated Ca^{2+} channels. Addition of glucose results in an inhibition of ATP-inhibited K^+ channels, which in turn gives rise to I_{Ca} and $I_{K,Ca}$. Thus, above 5 mM of glucose concentration, $I_{K,ATP}$ is not operative in the steady state (private communication with Dr. B. Ribalet), the outward current is primarily due to $I_{K,Ca}$, and the inward current is exclusively carried by Ca^{2+} ions through the V-gated Ca^{2+} channel. It should be emphasized here that $I_{K,ATP}$ is quite significant in the initial transient state (first 2–3 min after addition of glucose). Our model is concerned with the bursting "limit-cycle" regime, where $I_{K,ATP}$ is negligible (i.e., 15 min or so after addition of 5 mM or higher glucose concentration).

In terms of a Hodgkin-Huxley—like circuit model, the dynamics of the membrane potential V of such a system may be written as

$$4\pi r^2 C_m \, dV/dt = I_{Ca} + I_{K,Ca} + I_L, \quad (1)$$

where C_m is the membrane capacitance, r is the radius, and I_{Ca}, $I_{K,Ca}$, and I_L are, respectively, the voltage-gated calcium channel current, the Ca_i- and V-sensitive K^+ channel current, and the leak current. The leak current includes the currents due to the electrogenic pumps (e.g. Na/K and Ca-ATPase pumps) and the electrogenic exchange carrier systems (e.g., Na/Ca exchanger).

The ionic current carried by X ions may be expressed by a driving force multiplied by its conductance. The driving force is the difference between the membrane potential and reversal potential, which is the voltage at which no net current flows through the channel

$$I_X = g_X (V_X - V), \quad (2)$$

where X stands for K^+, Ca^{2+}, and leak ions, g_X is the conductance of X ions, and V_X is the reversal potential. The reversal potential for X ion can be conveniently expressed by the Nernst equation of the following form:

$$V_X = RT/Z_X F \ln ([X]_0/[X]_i), \quad (3)$$

where Z_X is the charge of X ion, RT carries its usual meaning, F is the Faraday constant, $[X]_0$ and $[X]_i$ are the X ionic concentrations for the extracellular and intracellular spaces, respectively. Since the concentrations of leak ions in the two phases are not known, we simply take V_L to be constant.

A single channel conductance is a measure of the permeability of X ions through a channel that permits X ions to pass through. It is equal to the total cell conductance g_X in Eq. 2 divided by the number of the channels. This channel consists of protein molecules whose rearrangements are responsible for the changes in conductance. The kinetics of the molecular rearrangements that cause conductance changes are complicated functions of membrane potential. The relaxation time for conformational changes is in the millisecond range and depends on the membrane potential. Thus, the conductances of the Ca^{2+} and K^+ channels depend sensitively on the voltage across the membrane as well as the relaxation time. A detailed knowledge of how the proteins sense gating and how this causes the channel to open or close is essential for successful mathematical modeling.

Unfortunately, detailed information on the kinetics of the V-gated Ca^{2+} channel and also the Ca_i-sensitive K^+ channel is not available in the literature. Thus, we are led to deduce a plausible kinetic mechanism for these two channels, based on the observed electrical activity of the β-cell. The spikes that occur during the active phase certainly demonstrate the importance of Ca^{2+} and K^+ permeability changes and moreover suggest that their

kinetics must follow a general shape given by the Hodgkin-Huxley Na^+ and K^+ kinetics. We assume that the V-gated calcium channel conductance, g_{Ca}, takes a form similar to the Hodgkin-Huxley Na^+ channel conductance and the Ca_i-sensitive K^+ channel conductance, $g_{K,Ca}$, takes a form similar to the Hodgkin-Huxley K^+ channel conductance. That is, g_{Ca} and $g_{K,Ca}$, which yield the spikes at the plateau potential of about -37 mV, take, respectively, the following expressions:

$$g_{K,Ca} = \bar{g}_{K,Ca}\, n^2 \tag{4}$$

$$g_{Ca} = \bar{g}_{Ca}\, m_\infty^2, \tag{5}$$

where $\bar{g}_{K,Ca}$ and $\bar{g}_{Ca}$ are, respectively, the maximum conductances of the Ca_i-sensitive potassium and voltage-gated calcium channels, n is the probability of opening of the Ca_i-sensitive K^+-channel, and m_∞ is the probability of the activation of the Ca^{2+} channel conductance in the steady state. Here, the assumption of rapid equilibrium for the m kinetics is due to the fact that the time required for the complete activation (i.e., ~15 ms) observed by Satin and Cook (1985) in cultured neonatal rat islet cells and by Findlay and Dunne (1985) in RINm5F is much shorter than the bursting periods (i.e., ~10 s, which is of our interest). We did not include the inactivation term "h" in g_{Ca}, because the experiment of Satin and Cook (1985) (and also private communication with Dr. Ribalet) conclusively shows that neither Ba^{2+} nor Ca^{2+} inactivates I_{Ca} completely within 40 ms. The voltage dependence of m_∞ in our model is that of Hodgkin and Huxley (1952) but V in Hodgkin Huxley is replaced by $-V + V_m$, where V_m is a constant that yields spikes at a plateau potential of about -37 mV (see Appendix A). Note that in the Hodgkin-Huxley model the exponents in Eqs. 4 and 5 are 4 and 3, respectively. Our choice of using the exponent 2 in Eq. 4 is that the open probability curves of Cook et al. (1984) and also Findlay et al. (1985*b*) suggest that the slopes of the open probability curves (at the half-maximal voltage) are not so steep, such that the second power may fit these curves better than the fourth. Our choice of the second power in Eq. 5 is that it is the lowest power that gives rise to the spike activity. We have done some computations (not shown here) using higher exponents for both g_{Ca} and $g_{K,Ca}$, but the use of higher exponents forced us to use larger $\bar{g}_{K,Ca}$ and $\bar{g}_{Ca}$ values than those in Table I.

The open probability, n, in Eq. 4 is a dynamic variable, with the relaxation time much larger than that of the m kinetics, and according to the Hodgkin-Huxley kinetics it should follow first-order kinetics

$$dn/dt = \lambda[n_\infty - n]/\tau_n, \tag{6}$$

where n_∞ is the steady state value of n, and τ_n is the relaxation time having the unit of milliseconds, and λ is a unitless time scaling factor. The voltage dependence of n_∞ and τ_n is that of Hodgkin and Huxley shifted by $-V_n - V_C$ mV on the voltage axis, i.e., V in the Hodgkin-Huxley expression replaced by $-V + V_n + V_C$. The sensitivity of $g_{K,Ca}$ on Ca_i comes in through V_C, which depends on Ca_i according to the relation (see Eq. 3 of Wong et al., 1982)

$$V_C = A \ln([Ca^{2+}]_i/1\ \mu M), \tag{7}$$

where A is a constant, which measures a sensitivity of the open probability to Ca_i (Cook et al., 1984). The inactivation of $g_{K,Ca}$ observed in the experiment of Findlay et al. (1985*b*) was not considered here because the experimental n_∞ curves suggest that the inactivation term becomes significant only in very high depolarization. The leak conductance, g_L, is taken to be constant.

In the β-cell, the cytosolic Ca^{2+} concentration is regulated by influx of extracellular Ca^{2+} ions entering the cell from the extracellular space and efflux of Ca_i ions disappearing from the transport systems located not only in plasma membrane but also in membranes of mitochondria, endoplasmic reticulum, and perhaps secretory granules. Using the rate law, the time derivative of $[Ca]_i$ may be expressed by

$$d[Ca^{2+}]_i/dt = f\{3I_{Ca}/4\pi r^3 F - k_{Ca}[Ca^{2+}]_i\}, \tag{8}$$

where f is a ratio between the dissociation constant and calcium binding buffer concentration (Chay, 1985*b*), and k_{Ca} is the rate constant of efflux of intracellular Ca^{2+} ions. A simple rate expression (i.e., $k_{Ca}[Ca^{2+}]_i$) was used for the efflux term in place of a Michaelis-Menten equation or Hill equation because the numerical solutions using either of these equations yield essentially the same results as reported here (Chay, 1985*b*). Moreover, since both the Michaelis-Menten or Hill equation make use of additional parameters (i.e., the Hill coefficient and the binding constant), we find no advantage to using either of them. Note that in our model glucose activates k_{Ca}, the efflux rate constant.

NUMERICAL RESULTS

As discussed in the previous section, our present model contains the following dynamic variables: (*a*) the membrane potential, V, whose variation with time is expressed as the sum of ionic currents carried by K^+ ions through a Ca_i-sensitive K^+ channel and by Ca^{2+} ions through a voltage-gated Ca^{2+} channel, and by the electrogenic pumps and carriers (see Eq. 1); (*b*) the probability of opening of the Ca_i-sensitive K^+ gate, n (see Eq. 6); and (*c*) the intracellular Ca^{2+} ionic concentration (see Eq. 8).

These differential equations were solved numerically on a DEC-10 computer (Digital Equipment Corp., Malboro, MA). A Gear algorithm (Hindmarsh, 1974) was used to solve the three equations, where we set both the absolute and relative error tolerances at 10^{-7}. This numerical ordinary differential equation solver is very well suited to solve stiff equations like ours. Most of the parameters (e.g., the radius r, the capacitance C_m, the extracellular and intracellular potassium concentrations, the extracellular

TABLE I
PARAMETER VALUES OF THE MODEL

Parameter	Unit	Numerical Value
C_m	$\mu F\ cm^{-2}$	1
$\bar{g}_{Ca}$	pS	250
$\bar{g}_{K,Ca}$	pS	1,500
g_L	pS	10
$[K^+]_0$	mM	5
$[K^+]_i$	mM	130
$[Ca^{2+}]_0$	mM	2.5
V_L	mV	−45
V_m	mV	−55
V_n	mV	−35
A	mV	−50
r	μm	6
f		1×10^{-4}
λ^{-1}		1.35
T	°K	310
k_{Ca}	ms^{-1}	0.04

calcium concentration, and the maximum conductances) in the model are not adjustable parameters, and hence we have obtained their values from experimental data on the β-cells. Those that were not available in β-cell experiments were estimated from experiments on other cells. The parameteric values used in our computation are listed in Table I. Whenever the values other than those in Table I are used, we listed them in the figure captions.

Fig. 1 illustrates the numerical solutions of the dynamics of β-cell electrical activity obtained with an increasing order of k_{Ca} from the top trace to the bottom. Bursts in the membrane potential (solid line) and oscillations in the intracellular calcium ionic concentration (dash line) result from a limit cycle oscillation. As can be seen in the figure, the burst mode in each panel has the following characteristics: When the glucose concentration is raised (i.e., an increase in k_{Ca}) beyond a certain value (i.e., $k_{Ca} > 0.007$), the membrane potential exhibits a typical pattern of a

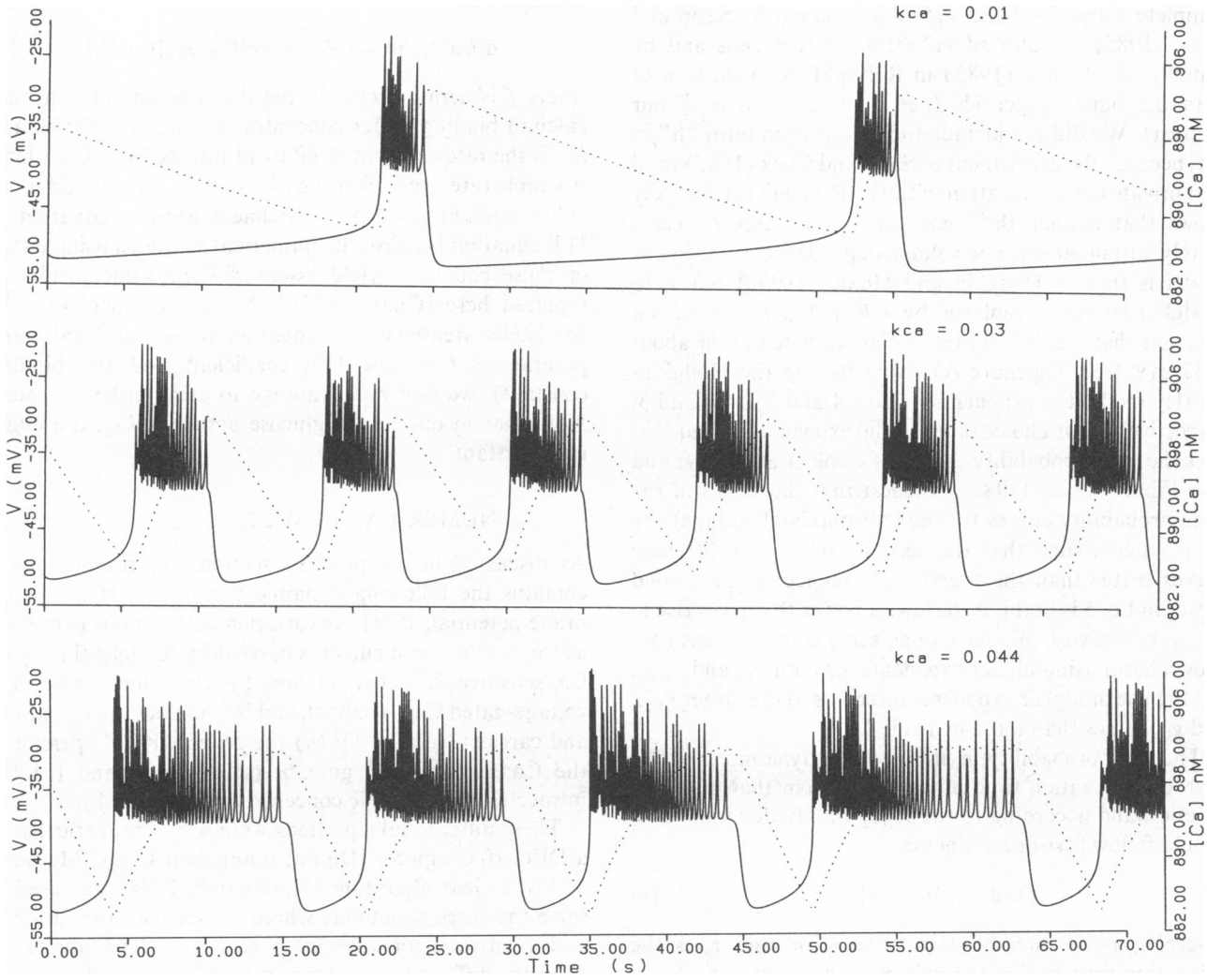

FIGURE 1 The burst behavior in response to increasing k_{Ca}, the Ca_i efflux rate constant. The solid line shows the membrane potential, and the dashed line shows the associated changes in the concentration of intracellular Ca^{2+} ions. Here, the values of k_{Ca}'s used for the computation are, from the top panel to the bottom, 0.01 ms^{-1}, 0.03 ms^{-1}, and 0.044 ms^{-1}, respectively.

burst, which includes a silent phase of repolarization followed by a rapid depolarization and continuous spike activity. The period of intracellular Ca^{2+} oscillations is identical to the burst period of membrane potential, although their shapes are quite different. At the beginning of a burst the Ca^{2+} concentration rises rapidly, peaking near the termination of the burst. This increase is caused by the action potential spikes, and during spiking Ca^{2+} ions flow into the cell from the perfusion medium. When $[Ca^{2+}]_i$ approaches the maximum level, the membrane potential falls abruptly to the minimum level of -52 mV. Note that the amplitude of $[Ca]_i$ oscillation is ~16 nM ($[Ca^{2+}]_{min} = 0.886$ and $[Ca^{2+}]_{max} = 0.902$). This is much smaller than that obtained using our previous model, which contains two separate K^+ channels, i.e., a voltage-gated, Ca_i-insensitive K^+ channel and a Ca_i-sensitive, voltage-independent K^+ channel (Chay and Keizer, 1983, 1985; Chay, 1985*b*). The amplitude of $[Ca]_i$ oscillation, however, could be made much bigger as A in Eq. 7 becomes smaller (see the top panel of Fig. 5).

In the burst regime, we observe that the shape of membrane potential depends very little on k_{Ca}: i.e., the maximum repolarization potential V_r is -51.9 mV; the plateau potential V_p is around -39 mV (at the beginning of the burst $V_p = -38.8$ and $V_{max} = -19.8$ at the end of the burst $V_p = -39.8$ and $V_{max} = -25.8$); the amplitude of spike potential is ~16 mV. The period of spikes at the beginning of the burst is ~100 ms, while it increases to ~400 ms at the termination of the burst. The above observations are consistent with the experimental results of

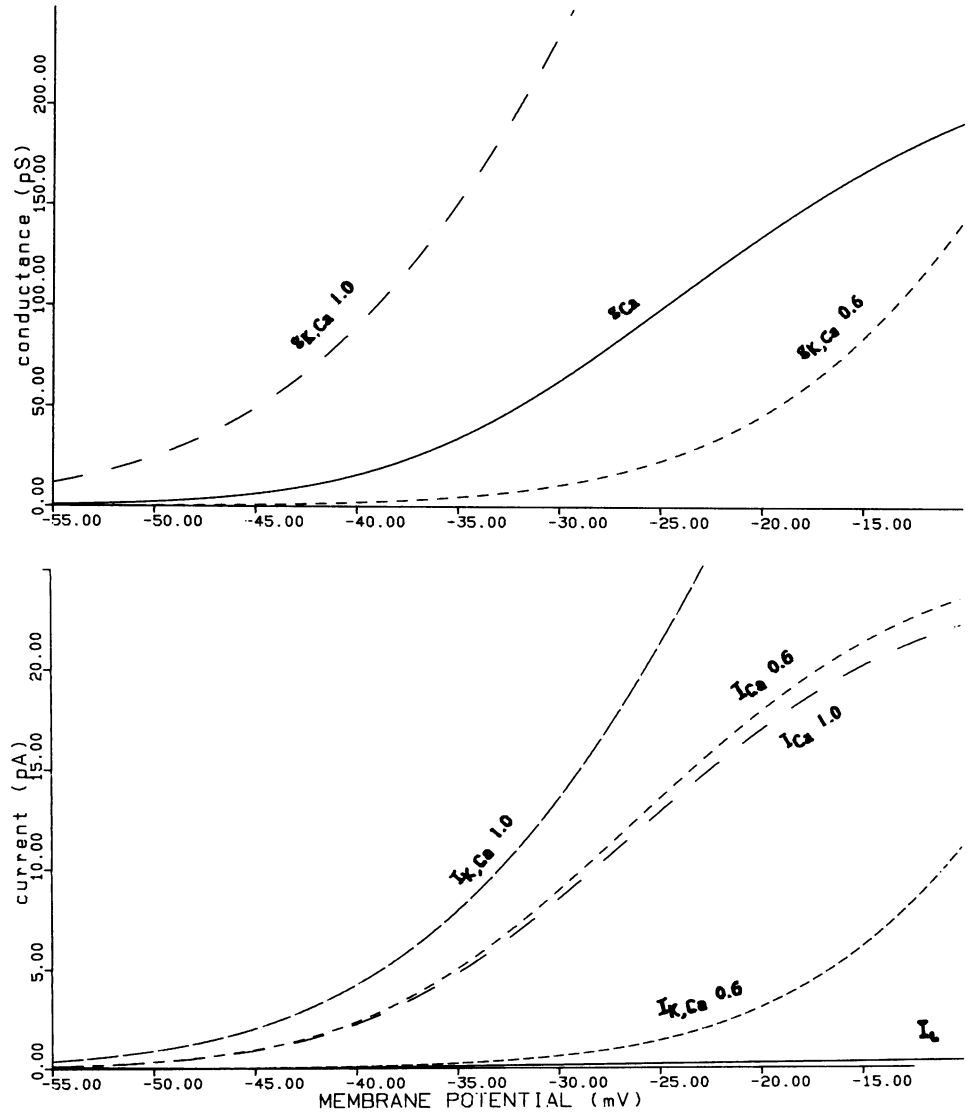

FIGURE 2 (*A*) The top panel shows a steady state voltage-gated Ca^{2+} contuctance g_{Ca}, and a steady state Ca_i-sensitive K^+ conductance $g_{K,Ca}$ at two different values of $[Ca^{2+}]_i$. The bottom panel shows the steady state calcium current $-I_{Ca}$ and steady state potassium current $I_{K,Ca}$, for two different values of $[Ca^{2+}]_i$. (*B*) The steady state $I_{K,Ca}$ v. membrane potential in response to changes of A (the *top* panel) and of V_n (the *bottom* panel), when $[Ca]_i$ is fixed at 0.8 μM.

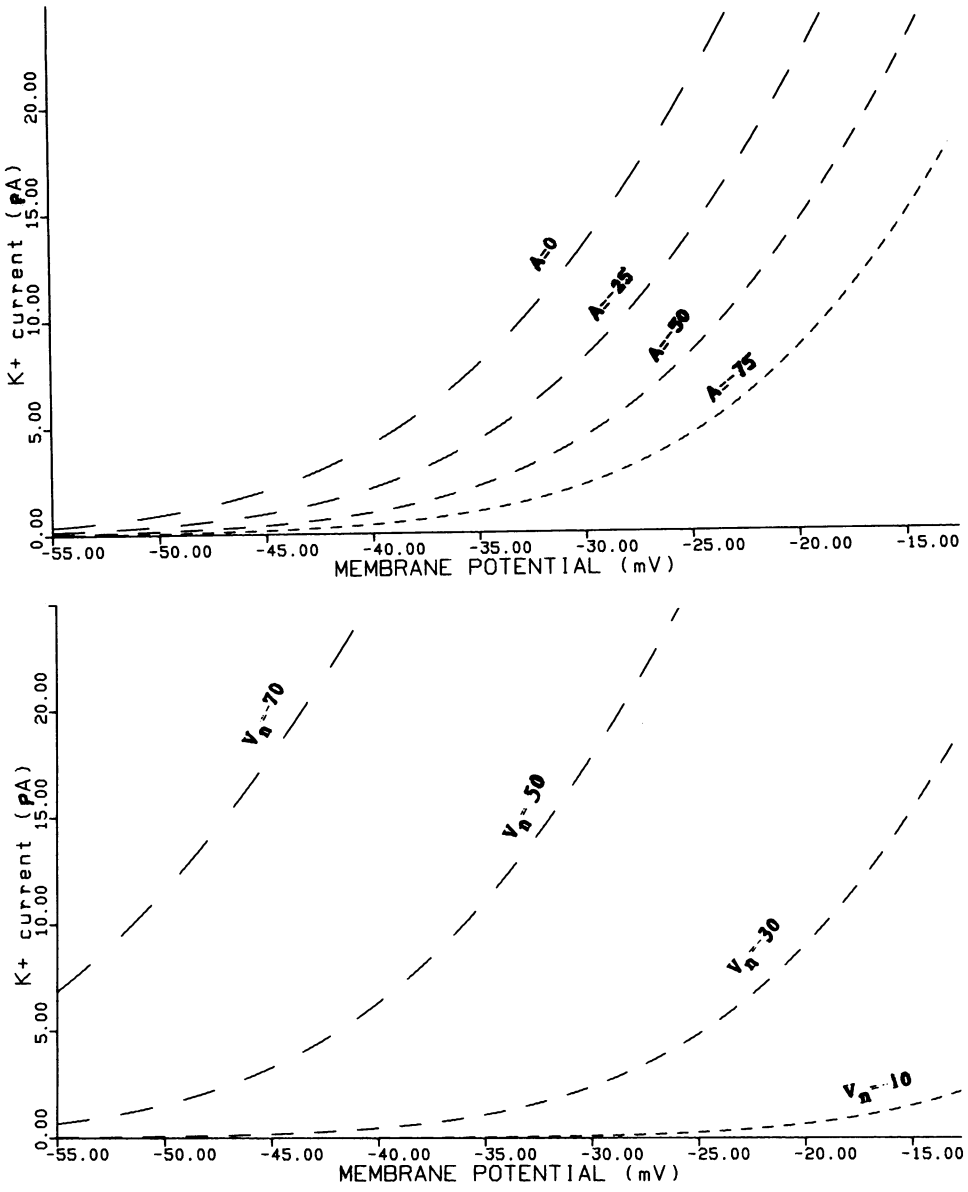

FIGURE 2 continued

Meissner and Preissler (1979). It is worthwhile to point out here that the lack of dependence upon k_{Ca} of the Ca-range and of the V-envelope (i.e., spike heights, plateau potential, and silent phase – max V and min V), during bursting could be seen nicely from Rinzel's mathematical analysis (Rinzel, 1985). This independence is true for changes in any parameters that appear only in the slow-variable equation, c.f. Eq. 8.

Although the shape of V bursts looks the same for all the k_{Ca} values, the duration of the silent phase becomes shorter and the active period becomes longer as k_{Ca} increases. Increasing k_{Ca} also results in a decrease in the burst periodicity. But as k_{Ca} is increased further the burst period increases again. Above a certain k_{Ca} value (i.e., $k_{Ca} > 0.045$ ms^{-1}), the bursts disappear entirely and only spikes remain. The k_{Ca} response on the active duration and the burst periodicity shown in Fig. 1 is consistent with the glucose dose response on the β-cell electrical activity observed experimentally (Beigelman et al., 1977; Ribalet and Beigleman, 1979). As shown in the bottom trace, the bursts near the onset of continuous spiking occur in a chaotic manner. This aperiodicity is known as determinitic chaos and is inherent in nonlinear dynamic systems like ours (Chay and Rinzel, 1985; Chay 1985*a*). Aperiodicity similar to this has been observed in experiments on the β-cells in high intermediate glucose concentration (Beigleman et al., 1977; Henquin et al., 1982).

In the top panel of Fig. 2 *A*, we show the two steady state conductances g_{Ca} and $g_{K,Ca}$, and in the bottom panel we show the steady state currents, $-I_{Ca}$ and $I_{K,Ca}$. Long dashes are obtained using $[Ca^{2+}]_i = 1.0$ μM, and short dashes using $[Ca]_i = 0.6$ μM. Note that $[Ca^{2+}]_i$ activates $I_{K,Ca}$ but

inhibits I_{Ca}. Note also that the two I_{Ca} curves fall between the two $I_{K,Ca}$ curves. This explains how the burst may arise from a system like ours. In the silent regime of the membrane potential, the V-gated calcium channel is quite inactive because of the low potential, and thus efflux of $[Ca]_i$ is larger than the influx (see Eq. 8). Indeed, in the earlier part of the silent regime, $-I_{K,Ca}$ is much larger than I_{Ca}, since $g_{K,Ca}$ depends not only on V but also on $[Ca^{2+}]_i$. As the cytosolic calcium ionic concentration decreases, the sum of the two currents, $I_{K,Ca} + I_{Ca}$, becomes smaller, finally reversing its sign near the termination of the silent phase, i.e., $-I_{K,Ca} > I_{Ca}$. This reversal of the sign, in turn, activates V-gated calcium channels. In the active phase, $I_{K,Ca} + I_{Ca}$ maintains the positive sign, i.e., I_{Ca} is larger than $-I_{K,Ca}$. As the Ca^{2+} channels open, calcium ions start to enter from the extracellular space; this gives rise to $[Ca^{2+}]_i$. An increase in $[Ca^{2+}]_i$ activates Ca_i-sensitive K^+ channels. When enough Ca^{2+} ions enter the cell, the sum, $I_{K,Ca} + I_{Ca}$, becomes essentially zero, and the active phase terminates when the sign is reversed. The cycle repeats again.

Fig. 2 *A* was obtained using $A = -50$ mV and $V_n = -35$ mV. $I_{K,Ca}$ depends not only on Ca_i but also on A and V_n. To show how the steady state $I_{K,Ca}$ depends on these parameteric values, we have shown, in Fig. 2 *B*, the steady state K^+ current-voltage relation, for various values of A and V_n. As shown in this figure, increasing $-A$ shifts the I-V curve to the right (top) and increasing $-V_n$ shifts the curve to the left (bottom).

The parameter A in Eq. 7, which measures a sensitivity of Ca_i on n_∞, is highly variable for different types of insulin secreting cells (Cook et al., 1984; Findlay et al., 1985) and even within the same cell type (Cook et al., 1984), ranging all the way from -17 to -57 mV. We have examined the effect of A on the bursting pattern by varying the value of A, and the result is presented in Fig. 3. Note that an

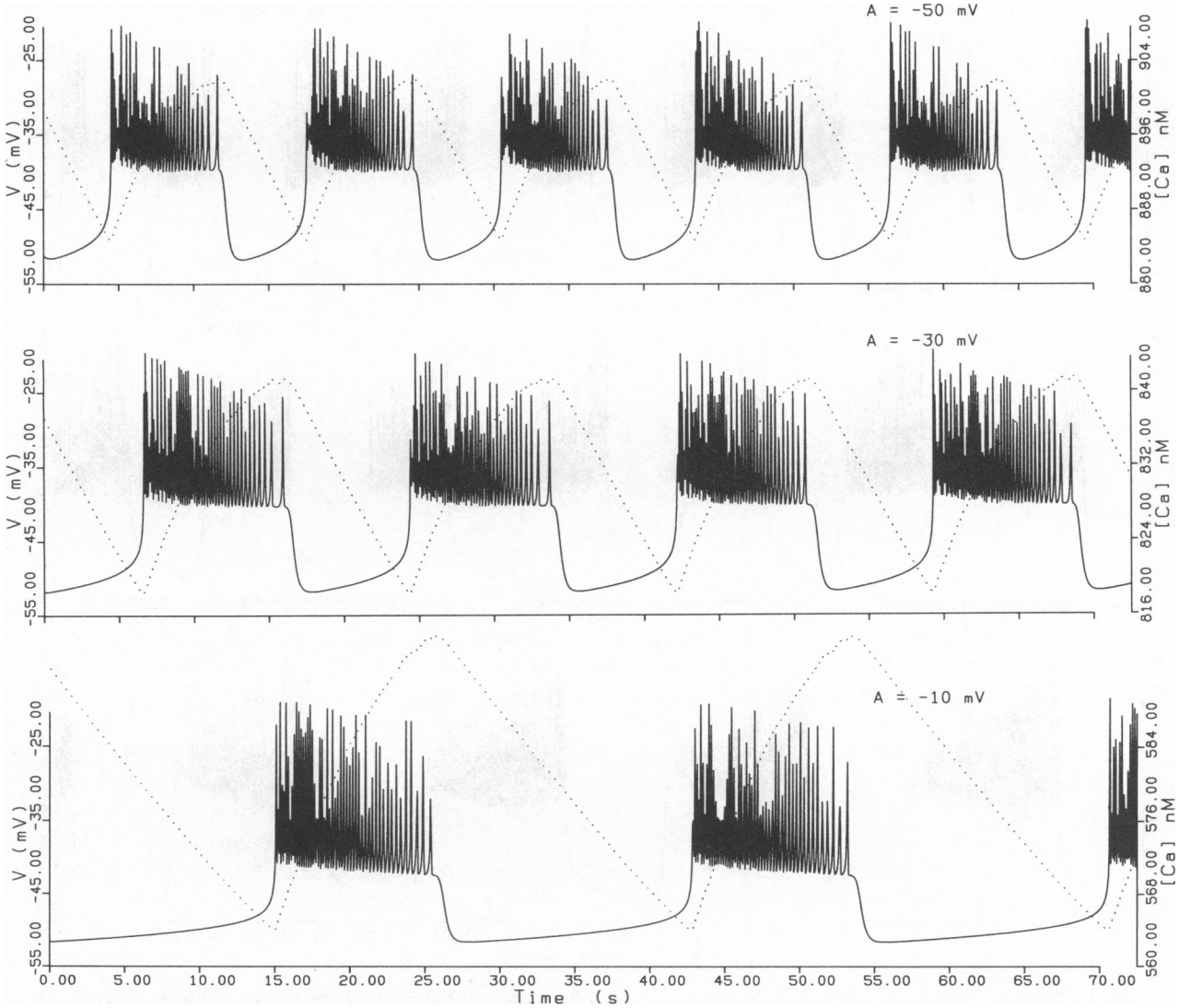

FIGURE 3 The burst behavior in response to decreasing $-A$, which measures the Ca_i sensitivity to $g_{K,Ca}$.

increase of $-A$ results in an increase of $[Ca^{2+}]_i$. Note, however, that this increase gives rise to a decrease in the amplitude Ca_i oscillations. Note also that the increase in $[Ca^{2+}]_i$ is such that $V_C = -A \ln[Ca^{2+}]_{mean}$ would remain always at ~6 mV (i.e., the sum $V_n + V_C$ is maintained at about −29 mV, if all other parameters are fixed at the values given in Table I). Due to this requirement, $[Ca]_i$ could never become greater than 1 μM, and as $-A$ becomes very large $[Ca]_i$ approach 1 μM. To have a value greater than 1 μM, then, V_n should be larger than −29 mV. For V_n larger than −29 mV, an increase in the magnitude of A results in a decreases $[Ca^{2+}]_i$, i.e., as $-A$ becomes larger $[Ca^{2+}]_i$ approaches 1 μM with a smaller amplitude of the oscillation. As shown in this example, V_n is a parameter that is responsible for raising a level of the intracellular Ca^{2+} concentration. On the other hand, A is a parameter which controls the amplitude of $[Ca]_i$ oscillations.

Cook et al. (1984) have shown that Ca^{2+}-activated K^+ channels in neonatal β-cells are sensitive to pH_i with the slopes of E_{50} (i.e., the half maximal V) v. pH_i curves ranging from −31 to −100 mV per pH unit. To study the effect of pH_i on the burst pattern, we assume that H^+ to be a competitive inhibitor to Ca_i, which affects the calcium binding constant. In our model, the calcium binding constant is modeled in V_n. The effect of varying V_n on bursting behavior is shown in Fig. 4. Note that an increase of V_n results in an increase in not only $[Ca]_i$ but also its amplitude. Note also that the increase induces an increase in the duration of the active phase similar to that evoked by higher concentrations of glucose. This is consistent with the observation made by Pace et al. (1983) and Eddlestone and Beigelman (1983) on islet β-cells in response to pH_i, which was made possible using the specific blockers of the Na/H exchange system.

Above two figures suggest how varying A and V_n

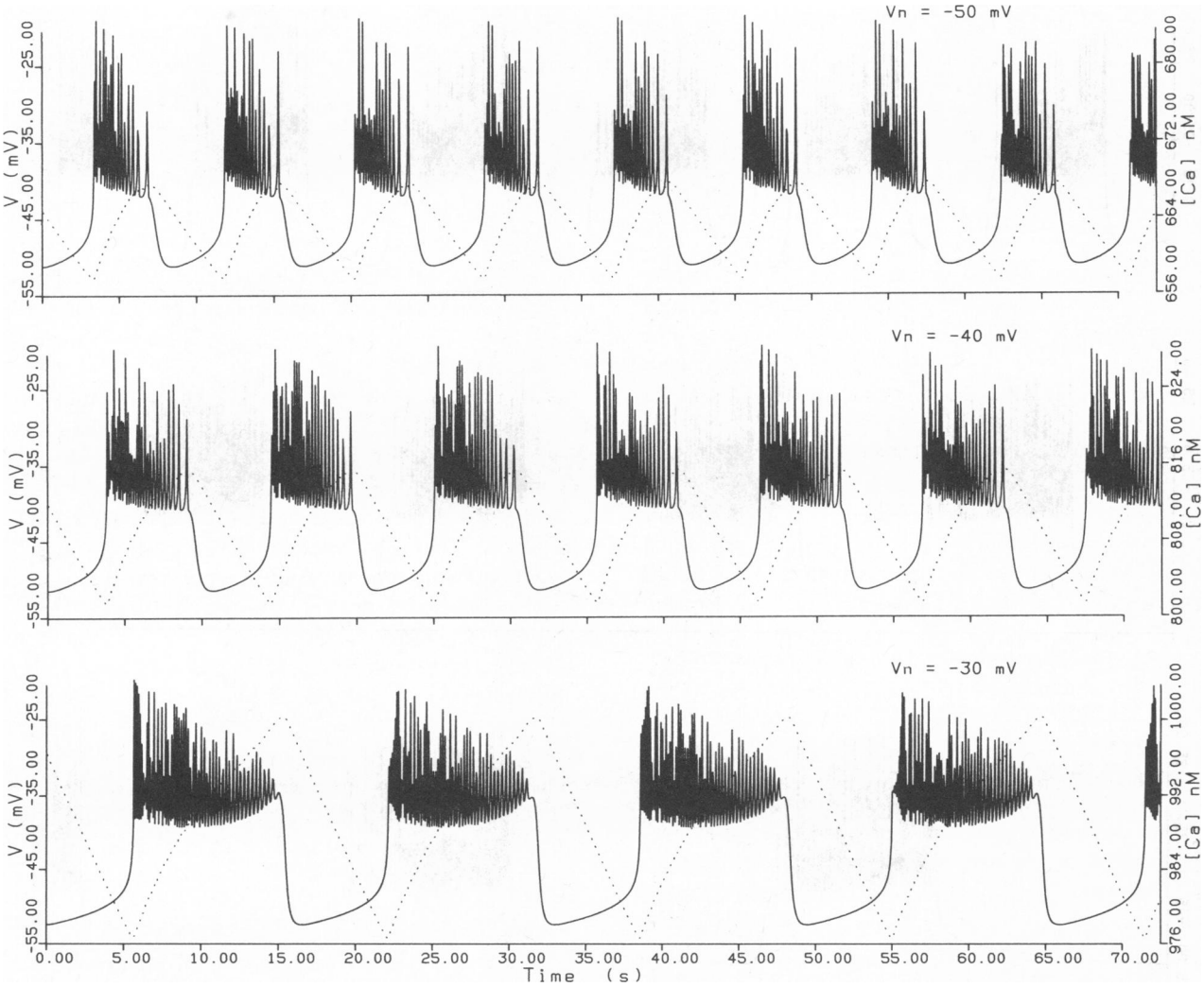

FIGURE 4 The burst behavior in response to decreasing $-V_n$, which measures the strength of the binding constant of Ca_i on the calcium-sensitive K^+ receptor protein.

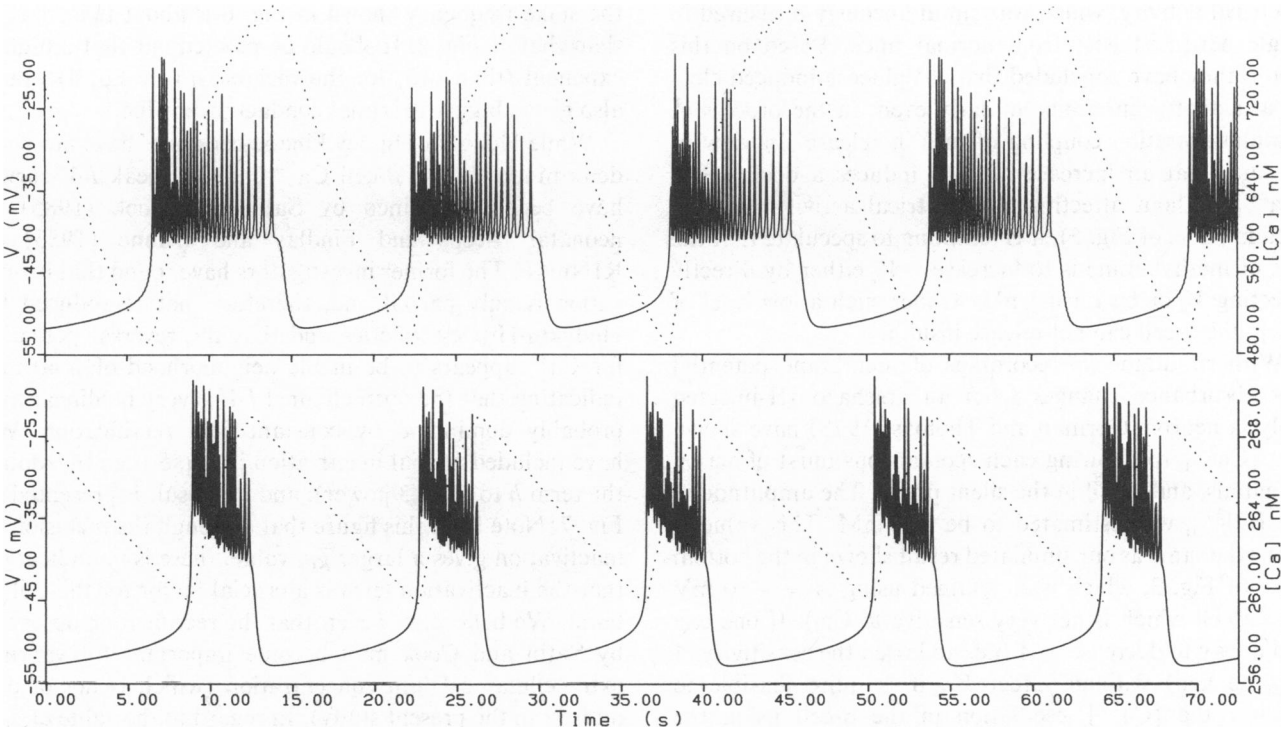

FIGURE 5 A large amplitude $[Ca]_i$ oscillation achieved by decreasing the magnitude of A and V_n (the *top* panel), a small amplitude achieved by increasing the magnitude of both A and V_n (the *bottom* panel). The parameters used for the top panel are $A = -1$ mV, $V_n = -30$ mV, $f = 2 \times 10^{-3}$, and those for the bottom panel are $A = -30$ mV, $V_n = -70$ mV, $f = 5 \times 10^{-5}$, $k_{Ca} = 0.1$, $\lambda = 1.2$.

controls the amplitude and magnitude of $[Ca^{2+}]_i$ oscillation. That is, an increase of the amplitude can be achieved by decreasing $-A$ and/or $-V_n$. Likewise, an increase of $[Ca^{2+}]_i$ can be achieved by increasing $-A$ and/or by decreasing $-V_n$. This effect is demonstrated in Fig. 5. Decreasing $-A$ and $-V_n$ to 1 mV and 30 mV, respectively, gives rise to a very large amplitude (i.e., 340 nM) and a relatively high $[Ca^{2+}]_i$, and increasing $-A$ and $-V_n$ to 30 mV and 70 mV, respectively, gives rise to a very small amplitude (i.e., 8 nM) and low $[Ca^{2+}]_i$. Implications of this result are that a cell whose $g_{K,Ca}$ is insensitive to Ca_i would yield a very large amplitude of $[Ca]_i$ oscillation during the electrical bursting (see the top panel) and that the electrical burst does not necessarily couple with a rise in the intracellular calcium concentration (the bottom panel).

DISCUSSION

With mathematical modeling, we exploit the crucial role that the Ca_i-activated K^+ channel plays on the electrical activity of insulin-secreting pancreatic β-cells. Our model reveals that the burst is, in fact, a consequence of the existence of Ca^{2+}-activated K^+ permeability, which, with voltage-gated Ca^{2+} permeability, triggers the spike activity and also terminates the active phase when a sufficient amount of cytosolic Ca^{2+} ions is raised. $I_{K,Ca}$ would dominate the silent phase of the burst. On the other hand, I_{Ca} would dominate the active phase, such that the influx of Ca^{2+} ions is larger than the efflux during the active phase, and the reverse is true during the silent phase. This is why the cytosolic Ca^{2+} concentration oscillates in synchrony with the membrane potential.

It appears that the role of the ATP-inhibited K^+-channel is to hold the membrane potential at the resting potential of about -70 mV, and thus an inhibition of $g_{K,ATP}$ (conductance of ATP-inhibited K^+-channel) gives rise to an activation of the voltage-gated Ca^{2+} channel and Ca_i-sensitive K^+ channel activities. At the resting state, the cytosolic calcium concentration is very low, because the Ca^{2+} channel gate is completed closed. The primary role of glucose on the electrical activity is, then, to inhibit the ATP-inhibited K^+-channel activity, so as to activate both voltage-gated Ca^{2+} channels and Ca_i-sensitive K^+ channels. The secondary role of glucose is to activate efflux of Ca_i, as our simulation result in Fig. 1 suggests. The fact that a decrease in $-V_n$ gives rise to a long active phase and an increase in $[Ca^{2+}]_i$ (see Fig. 4) raises an interesting possibility that the initial rich active phase observed in the transient biphasic phase may owe its origin to cytoplasmic acidification as a result of mitochondrial sequestration. The nadir observed in insulin release (Charles et al., 1975) may then be a result of a rise in $[Ca^{2+}]_i$, due to a decrease in pH_i.

Lebrun et al. (1985) have observed that methylamine inhibits glucose-induced insulin release without affecting

electrical activity, which was simultaneously measured in single perifused islet from normal mice. Based on this result, they have concluded that the glucose-induced electrical activity represents an early event in the process of stimulus-secretion coupling of insulin release. In view of the fact that an increase of $-V_n$ induces a decrease of $[Ca^{2+}]_i$ without affecting the electrical activity (see the bottom panel of Fig. 5), it is tempting to speculate that the role of methylamine is to increase $-V_n$ either by directly affecting V_n or by raising pH_i. Under such a low level of $[Ca]_i$, the β-cell can not release insulin.

With simultaneous recordings of membrane potential and absorbance changes from an arsenazo III-injected Aplysia neuron, Gorman and Thomas (1978) have shown that $[Ca^{2+}]_i$ rose during each spontaneous burst of action potentials, and it fell in the silent phase. The amplitude of the $[Ca^{2+}]_i$ was estimated to be ~50 nM. This value is about the same as our simulated result shown in the bottom trace of Fig. 3, which was obtained using $A = -10$ mV (i.e., a cell which is not very sensitive to Ca_i). If one can find a way to decrease $-A$ (i.e., to lessen the sensitivity of $g_{K,Ca}$ to Ca_i) without affect V_n, it is quite feasible to monitor the $[Ca^{2+}]_i$ oscillation in the β-cell using the fluorescent dyes such as quin2.

The value of 250 pS was estimated from measurements of the single Ca_i-sensitive K^+ channel conductance of the islet cells (Cook et al., 1984; Findlay et al., 1985). No estimation was made for the number of these channels per cell, however. Measurements in pancreatic acinar tissue suggest that there may be as many as 45 channels per cell (Maruyama et al., 1983). Using these values, we estimate the maximum conductance to be ~11.3 nS. This way of estimating the maximum conductance value, however, gives ~50% larger than the actual $\bar{g}_{K,Ca}$. Taking this into consideration, we find $\bar{g}_{K,Ca}$ to be 5.7 nS, which is about four times larger than the value we have used in our computation (see Table I). To demonstrate that we may have easily doubled the value without affecting our results, we have presented, in Fig. 6, the electrical burst, which was obtained using $\bar{g}_{K,Ca} = 3$nS. The major difference between this figure and that shown in the top panel of Fig. 2 is that the spike frequency shown in Fig. 6 is about twice larger than that of Fig. 2. It should be pointed out that a higher exponent (than two) for the variable n (see Eq. 4) would also give a bigger maximal conductance value.

While Hodgkin-Huxley kinetic constants have not been determined for the β-cell Ca^{2+} channel, peak I-V curves have been determined by Satin and Cook (1985) in neonatal β-cells and Findlay and Dunne (1985) in RINm5F. The former investigators have found that inactivation is only partial and, therefore, not reproduced by Hodgkin-Huxley kinetics and that the reversal potential for Ca^{2+} appears to be in the neighborhood of +40 mV indicating that the open channel I-V is very nonlinear and probably dominated by constant field rectification. We have included partial inactivation in Eq. 5 (i.e., by adding the term h to the 0.3 power), and the result is presented in Fig. 7. Note from this figure that although the inclusion of inactivation gives a larger $\bar{g}_{Ca}$ value, there is no indication that the inactivation term is a crucial factor for the cell to burst. We believe, however, that the rectification observed by Satin and Cook may become important for varying extracellular calcium concentration (which is not of our interest in the present study). In regard to the value of $\bar{g}_{Ca}$, we have used $\bar{g}_{Ca} = 250$ pS in our computation (see Table I). The upper bound of the single calcium conductance was estimated to be 5 pS from the voltage noise measurements across the pancreatic β-cell membrane (Atwater et al., 1981). Assuming that an estimation of the maximum channel conductance from a single channel conductance yields a value larger by a factor of 30%, we find that there are at least 170 calcium channels per β-cell. Inclusion of a mild inactivation term (see the caption of Fig. 7) gives a much larger number of the channels (using the maximum conductance value of 900 pS we estimate the minimum number of calcium channels to be about 600 per cell).

We believe that the kinetics of g_{Ca} and $g_{K,Ca}$ given in Eqs. 4 and 5 are not unique (for the cell to burst). We believe, however, that the true channel activity (in the steady state) has a shape similar to I_{Ca} and $I_{K,Ca}$ shown in Fig. 2. That is, both g_{Ca} and $g_{K,Ca}$ have a sigmoidal shape; in physiological $[Ca^{2+}]_i$ they are steeply rising functions of membrane

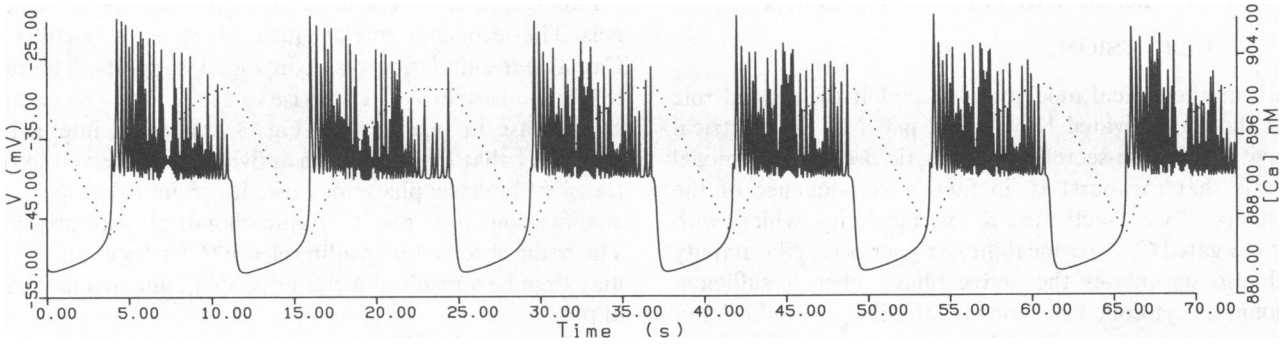

FIGURE 6 This figure compares the bursting behaviors with those shown in the top panel of Fig. 3 when g_x's are doubled by a factor of two. Also, k_{Ca} was doubled, and f and λ (i.e., 0.68) were halved.

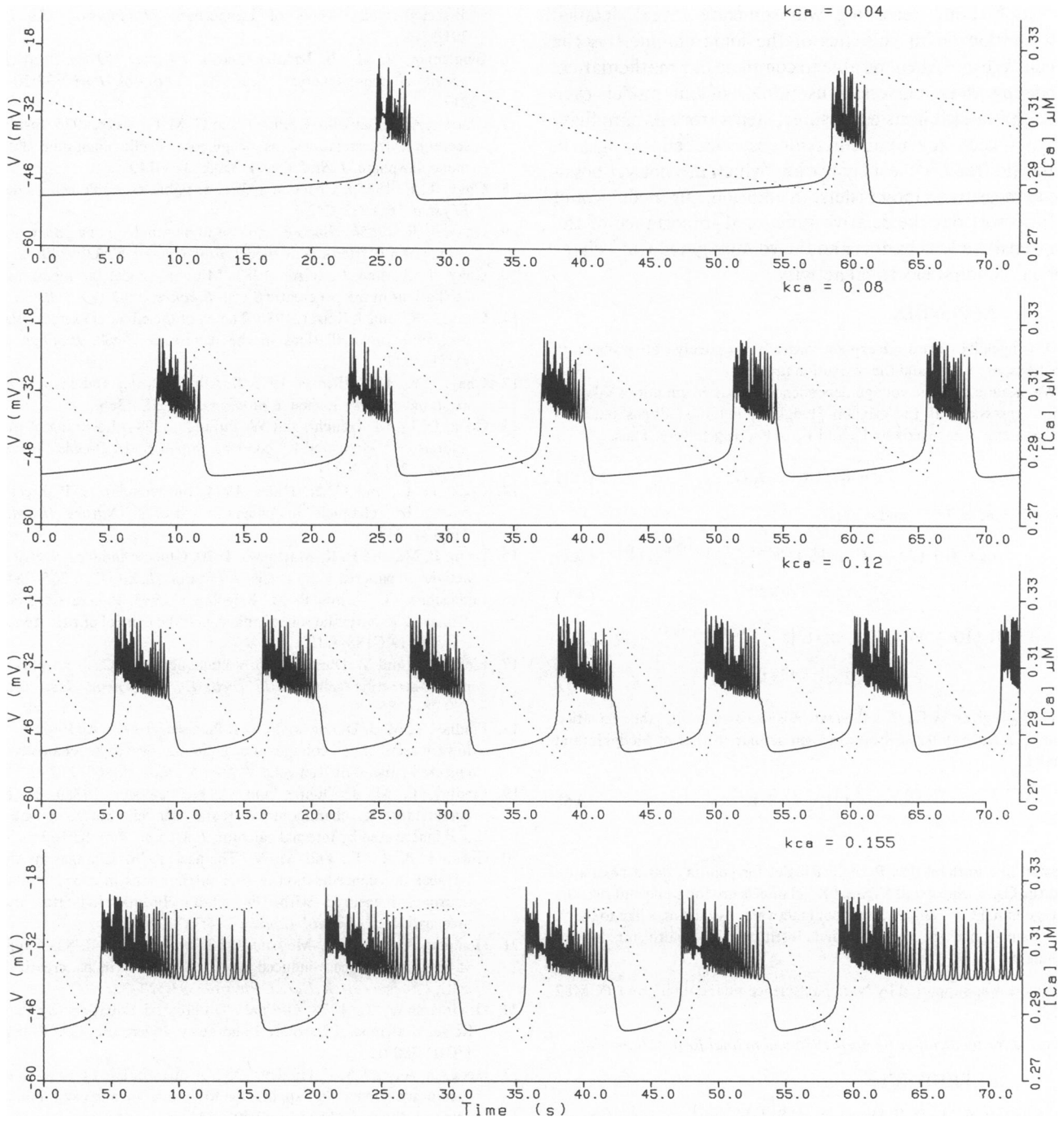

FIGURE 7 The burst behavior obtained by adding the inactivation term $h_\infty^{0.3}$ to Eq. 5. Here, the values of k_{Ca}'s used for the computation are, from the top panel to the bottom, 0.04 ms^{-1}, 0.08 ms^{-1}, 0.12 ms^{-1}, and 0.155 ms^{-1}, respectively. Those parameteric values that are different from Appendix B are: $\bar{g}_{Ca}$ = 900 pS, $\bar{g}_{K,Ca}$ = 1,300 pS, g_L = 20 pS, $V_n = -37$ mV, $V_m = -50$ mV, $A = -5$ mV, $\lambda^{-1} = 1.3$, and $f = 2 \times 10^{-4}$.

potential near -35 mV; $g_{K,Ca}$ should be activated by $[Ca^{2+}]_i$; on the other hand, I_{Ca} should be inhibited either by the "h" kinetics or by $[Ca^{2+}]_i$. Perhaps, it is worth mentioning here that $I_{K,Ca}$ in Fig. 2 has about the same magnitude and shape as two potassium currents (Ca_i-sensitive, V-insensitive K^+ channel and V-gated, Ca_i-insensitive K^+ channel currents) combined in our earlier model (Chay and Keizer, 1983, 1985; Chay, 1985*a*, *b*). There is no direct experimental evidence to verify the existence of the two separate K^+ channels. Instead, the single channel recording of Cook et al. (1984) and Findlay et al. (1985) suggests that these two channels are indeed identical.

Accurate determination of the channel properties is vital to our understanding of the role of $[Ca^{2+}]_i$ on the insulin release mechanism. Continuing refinements of resolution

of patch-clamp recording will someday reveal detailed information on the kinetics of the ionic channels in the β-cell. We will, then, be able to complete our mathematical modeling. Nevertheless, a usefulness of our model, even though it is still in its early stage, stems from its simplicity and its accuracy to predict glucose-induced changes in cytosolic free Ca^{2+} concentration, which are not yet possible to measure in intact islets. In addition, our model would help to sort out the relative functional importance of the Ca_i-sensitive K^+ channel and the voltage-gated Ca^{2+} channel on the burst electrical activity.

APPENDIX

In this appendix we provide explicit forms for the steady state probability functions, m_∞ and n_∞ and the relaxation time τ_n.

We assume that the voltage dependencies of these quantities take the same expressions as the original Hodgkin-Huxley equations but V is shifted along voltage axis by V_m and $V_n + V_C$, respectively. Thus,

$$Y_\infty = \alpha_y/(\alpha_y + \beta_y), \tag{A1}$$

where Y_∞ stands for m_∞ and n_∞, and

$$\alpha_m = 0.1\ (25 - V + V_m)/\{e^{(-V + V_m + 25)/10} - 1\} \tag{A2}$$

$$\beta_m = 4e^{(-V + V_m)/18} \tag{A3}$$

$$\alpha_n = 0.01\ (10 - V + V_n + V_C)/\{e^{-V + V_n + V_C + 10)/10} - 1\} \tag{A4}$$

$$\beta_n = 0.125e^{(-V + V_n + V_C)/80}, \tag{A5}$$

where V_C is given by Eq. 7 in the text. We also assume that the relaxation time τ_n in Eq. 6 follows the expression similar to that of Hodgkin and Huxley

$$\tau_n = 1/(\alpha_n + \beta_n). \tag{A6}$$

I would like to thank Dr. Bernald Ribalet for pointing out a possibility that the Ca_i-sensitive and V-gated K^+ channels are the same and that the voltage-gated Ca^{2+} channel does not inactivate. I would also like to thank Dr. John Rinzel at the National Institutes of Health for helpful comments.

This work was supported by National Science Foundation grant PCM82 15583.

Received for publication 14 April 1986 and in final form 5 June 1986.

REFERENCES

1. Ashcroft, F. M., D. E. Harrison and S. J. H. Ashcroft. 1984. Glucose induces closure of single potassium channels in isolated rat pancreatic β-cells. *Nature (Lond.).* 312:446–448.
2. Atwater, I., C. M. Dawson, G. T. Eddlestone, and E. Rojas. 1981. Voltage noise measurements across the pancreatic β-cell membrane: calcium channel characteristics. *J. Physiol. (Lond.).* 313:195–212.
3. Atwater, I., C. M. Dawson, B. Ribalet, and E. Rojas. 1979. Potassium permeability activated by intracellular calcium ion concentration in ithe pancreatic B-cell. *J. Physiol. (Lond.).* 278:575–588.
4. Atwater, I., C. M. Dawson, A. Scott, G. Eddlestone, and E. Rojas. 1980. The nature of the oscillatory behavior in electrical activity for pancreatic β-cell. *In* Biochemistry Biophysics of the Pancreatic β-cell. Georg Thieme Verlag, New York. 100–107.
5. Atwater, I., E. Rojas, and A. Scott. 1979. Simultaneous measurements of insulin release and electrical activity from single microdissected mouse islets of Langerhans. *J. Physiol. (Lond.).* 291:57P.
6. Beigelman, P. M., B. Ribalet, and I. Atwater. 1977. Electrical activity of mouse pancreatic beta-cells. *J. Physiol. (Paris).* 73:201–217.
7. Charles, A., J. Lawecki, R. Pictet, and G. M. Grodsky. 1975. Insulin secretion: Interrelationships of glucose, cyclic adenosine 3′:5′-monophosphate. *J. Biol. Chem.* 250:6134–6140.
8. Chay, T. R. 1985*a*. Chaos in a three-variable excitable cell model. *Physica.* 16D:233–242.
9. Chay, T. R. 1985*b*. Glucose response to bursting-spiking pancreatic β-cells by a barrier kinetic model. *Biol. Cybern.* 52:339–349.
10. Chay, T. R., and J. Keizer. 1983. Minimal model for membrane oscillations in the pancreatic β-cell. *Biophys. J.* 42:181–190.
11. Chay, T. R., and J. Keizer. 1985. Theory of the effect of extracellular potassium on oscillations in the pancreatic β-cell. *Biophys. J.* 48:815–827.
12. Chay, T. R., and J. Rinzel. 1985. Bursting, beating, and chaos in an excitable membrane model. *Biophys. J.* 47:357–366.
13. Cook, D. L., M. Ikeuchi, and W. Fujimoto. 1984. Lowering of pH_i inhibits Ca^{2+}-activated K^+ channels in pancreatic B-cells. *Nature (Lond.).* 311:269–271.
14. Cook, D. L., and C. N. Hales. 1984. Intracellular ATP directly blocks K^+ channels in pancreatic B-cells. *Nature (Lond.).* 311:271–273.
15. Dean, P. M., and E. K. Matthews. 1970. Glucose-induced electrical activity in pancreatic islet cells. *J. Physiol. (Lond.).* 210:255–264.
16. Eddlestone, G. T., and P. M. Beigelman. 1983. Pancreatic β-cell electrical activity: the role of anions and the control of pH. *Am. J. Physiol.* 13:C188–C197.
17. Findlay, I., and M. Dunne. 1985. Voltage-activated Ca^{2+} currents in insulin-secreting cells. *FEBS (Fed. Eur. Biochem. Soc.) Lett.* 189:281–285.
18. Findlay, I., M. J. Dunne, and O. H. Petersen. 1985*a*. ATP-sensitive inward rectifier and voltage- and calcium-activated K^+ channels in cultured pancreatic islet cells. *J. Membr. Biol.* 88:165–172.
19. Findlay, I., M. J. Dunne, and O. H. Petersen. 1985*b*. High-conductance K^+ channel in pancreatic islet cells can be activated and inactivated by internal calcium. *J. Membr. Biol.* 83:169–175.
20. Gorman, A. L. F., and M. V. Thomas. 1978. Changes in the intracellular concentration of free calcium ions in a pace-maker neurone, measured with the metallochromic indicator dye arsenazo III. *J. Physiol. (Lond.).* 275:357–376.
21. Henquin, J. C., H. P. Meissner, and W. Schmeer. 1982. Cyclic variations of glucose-induced electrical activity in pancreatic B cells. *Pfluegers Arch. Eur. J. Physiol.* 393:322–327.
22. Hindmarsh, A. C. 1974. Ordinary Differential Equations Systems Solver. Lawrence Livermore Laboratory. Livermore, CA. Report UCID-30001.
23. Hodgkin, A., and A. F. Huxley. 1952. A quantitative description of membrane current and application to conduction and excitation in nerve. *J. Physiol. (Lond.).* 117:500–544.
24. Lebrun, P., I. Atwater, L. M. Rosario, A. Herchuelz, and W. J. Malaisse. 1985. Dissociation by methlamine of insulin release from glucose-induced electrical activity in isolated mouse islets of Langerhans. *Metabolism.* 34:1122–1127.
25. Maruyama, Y., O. H. Petersen, P. Flanagan, and G. T. Pearson. 1983. Quantification of Ca^{2+}-activated K^+ channels under hormonal control in pig pancrease acinar cells. *Nature (Lond.).* 305:228–232.
26. Matthews, E. K., and Y. Sakamoto. 1975. Electrical characteristics of pancreatic islet cells. *J. Physiol. (Lond.).* 246:421–437.
27. Meissner, H. P., and M. Preissler. 1979. Glucose-induced changes of pancreatic B-cells: Their significance for the regulation of insulin release. *In* Treatment of early diabetes. R. A. Camerini-Davalos and B. Hanover, editors. Plenum Publishing Corp., New York. 97–107.

28. Meissner, H. P., and M. Preissler. 1980. Ionic mechanisms of the glucose-induced membrane potential changes in B-cells. *In* Biochemistry and Biophysics of the Pancreatic-B-Cell. Springer-Verlag, New York. 91–99.

29. Meissner, H. P., and H. Schmelz. 1974. Membrane potential of beta-cells in pancreatic islets. *Pfluegers Arch. Eur. J. Physiol.* 351:195–206.

30. Pace, C. S., J. T. Tarvin, and J. S. Simith. 1983. Stimulus-secretion coupling in β-cells: modulation by pH. *Am. J. Physiol.* 244:E3–E18.

31. Petersen, O. H., and Y. Maruyama. 1984. Calcium-activated potassium channels and their role in secretion. *Nature (Lond.).* 307:693–696.

32. Ribalet, B., and P. M. Beigelman. 1979. Cyclic variation of K^+ conductance in pancreatic β-cells: Ca^{2+} and voltage dependence. *Am. J. Physiol.* 237:C137–C146.

33. Rinzel, J. 1985. Bursting oscillations in an excitable membrane model. in Lecture notes in mathematics. A. Dold and B. Eckmann, editors. Ordinary and partial differential equations. Proceedings of the eighth conference held at Dundee, Scotland, June 25–29, 1984. Springer-Verlag Berlin, Hedelberg, New York, Tokyo.

34. Rorsman, P., H. Abrahamsson, E. Gylfe, and B. Hellman. 1984. Dual effects of glucose on the cytosolic Ca^{2+} activity of mouse pancreatic β-cells. *FEBS (Fed. Eur. Biochem Soc.) Lett.* 170:196–200.

35. Satin, L. S., and D. L. Cook. 1985. Voltage-gated Ca^{2+} current in pancreatic B-cells. *Pfluegers Arch.* 404:385–387.

36. Scott, A. M., I. Atwater, and E. Rojas. 1981. A method for the simultaneous measurement of insulin release and B cell membrane potential in single mouse islets of Langerhans. *Diabetologia.* 21:470–475.

37. Wollheim, C. B., and T. Rozzan. 1984. Correlation between cytosolic free Ca^{2+} and insulin release in an insulin-secreting cell line. *J. Biol. Chem.* 259:2262–2267.

38. Wong, B. S., H. Lecar, M. Adler. 1982. Single calcium-dependent potassium channels in clonal anterior pituitary cells. *Biophys. J.* 39:313–317.